Supplementary Calculation

Dependency of the steady-state methane concentration in the epilimnion on the half-saturation constant

We consider a well-mixed epilimnion that contains a microbial species B with biomass expressed in µM C that grows on a single carbon (C) substrate S at concentrations expressed in µM C according to the Monod growth kinetics. Furthermore, we assume that the substrate is released from the sediment of the lake and that the concentration gradient from the sediment to the epilimnion has reached a steady state. In this case, we have a constant volumetric flux F_S in µM C d^{-1} into the epilimnion.

Without microbial growth, exchange with the atmosphere and substrate consumption, the change of the substrate concentration in the epilimnion is simply

$$\frac{dS}{dt} = F_S \tag{1}$$

According to the Monod kinetics, the growth rate r in d^{-1} of the microbial species is:

$$r = V_{max}\frac{S}{S + K_M} \tag{2}$$

where V_{max} is the maximum growth rate in d^{-1} and K_M the half-saturation constant in µM.

Considering a mortality rate m in d^{-1} and a substrate use efficiency y, the temporal change of the bacterial species is:

$$\frac{dB}{dt} = (y \cdot r - m)B \tag{3}$$

Due to the growth of the bacterial species, the substrate concentration in the well-mixed epilimnion decreases with a rate of $-rB$ and the complete system of differential equations is:

$$\frac{dS}{dt} = F_S - rB \tag{4}$$

$$\frac{dB}{dt} = (y \cdot r - m)B$$

For an equilibrium estimate, we assume steady-state for the substrate concentration but not for the biomass:

$$\frac{dS}{dt} = 0 = F_S - rB \tag{5}$$

By rearranging equation 5, we get an equilibrium substrate concentration of:

$$S^{eq} = \frac{F_S \cdot K_M}{B \cdot V_{max} - F_S} \quad (6)$$

Estimated equilibrium concentration in the epilimnion of Lake Rotsee: In the epilimnion, we measured an average K_M of 1.8 µM. With a cellular carbon content of 0.42 pmole C cell^{-1} (Oswald et al., 2015; Posch et al., 2001; Romanova and Sazhin, 2010) and average cell numbers of 0.1x10^5 – 2.5x10^5 cells mL^{-1}, we estimate average biomass of 4 – 105 µM C. In the epilimnion we measured an average maximum methane oxidation rate of about 4 fmole h^{-1} cell^{-1}. Using the above cellular carbon content, this converts to a maximum methane oxidation rate of 0.2 day^{-1}. Based on model work (Zimmermann et al., 2019), the median volumetric flux of methane into the epilimnion is 5 µM day^{-1}.

Inserting these values into equation 6 results in an equilibrium methane concentration of 0.6 – 1.5 µM, depending on the amount of biomass (lower equilibrium concentrations with higher biomass). Compared to the K_M of 1.8 µM used in the calculation, this demonstrates that the expected methane concentration tends to be lower than the half-saturation constant K_M.

Supplementary Figures

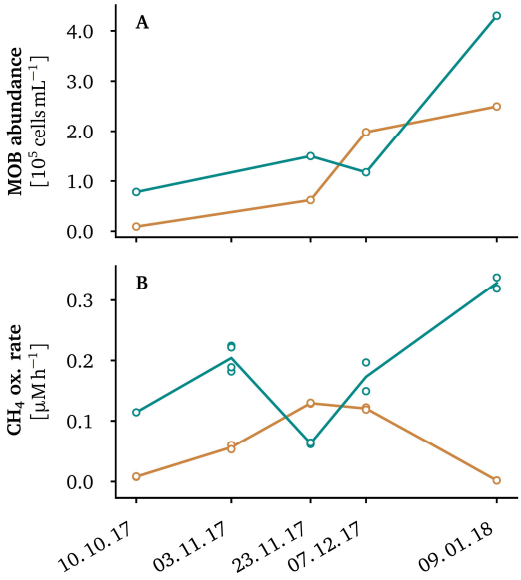

Supplementary Figure 1

Cell numbers (A) and methane oxidation rates (B) recorded at sampling dates above (orange) and below (cyan) the oxycline. For the methane oxidation rates, we measured at an additional date in the beginning of November.

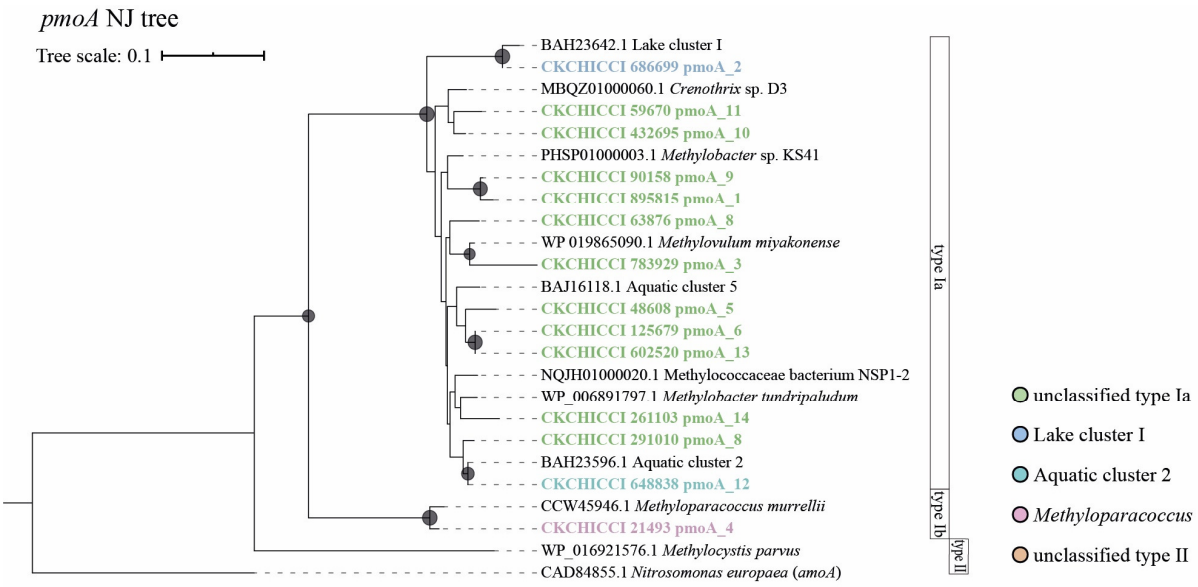

Supplementary Figure 2

Phylogenetic placement of MOB *pmoA* amino acid sequences found in this study with reference sequences from cultivated and uncultivated MOB. The Neighbor joining (NJ) tree was inferred with MEGA7 (Kumar et al., 2016) based on partial *pmoA* amino acid sequences (131 positions) and Poisson correction method. Grey dots indicate nodes with a bootstrap value above 0.7 (10 000 bootstrap replicates). Colors are specific to the taxonomic classification and correspond to the colours used in Figure 3a of the main text. Reference sequences are given with accession numbers to the left of the species name, or cluster name (Knief, 2015) in case of uncultivated MOB. To the left of the sequences found in this study, gene identifiers are shown, corresponding to the list in the supplementary file. The numbering of *pmoA* variants is arbitrary and was done to have simple and unique identifiers for the different *pmoA* variants. The scale bar represents changes per amino acid position. The tree was visualized with iTOL (Letunic and Bork, 2007) and rooted with the outgroup sequence of the ammonia monooxygenase (*amoA*) of *Nitrosomonas europaea.*

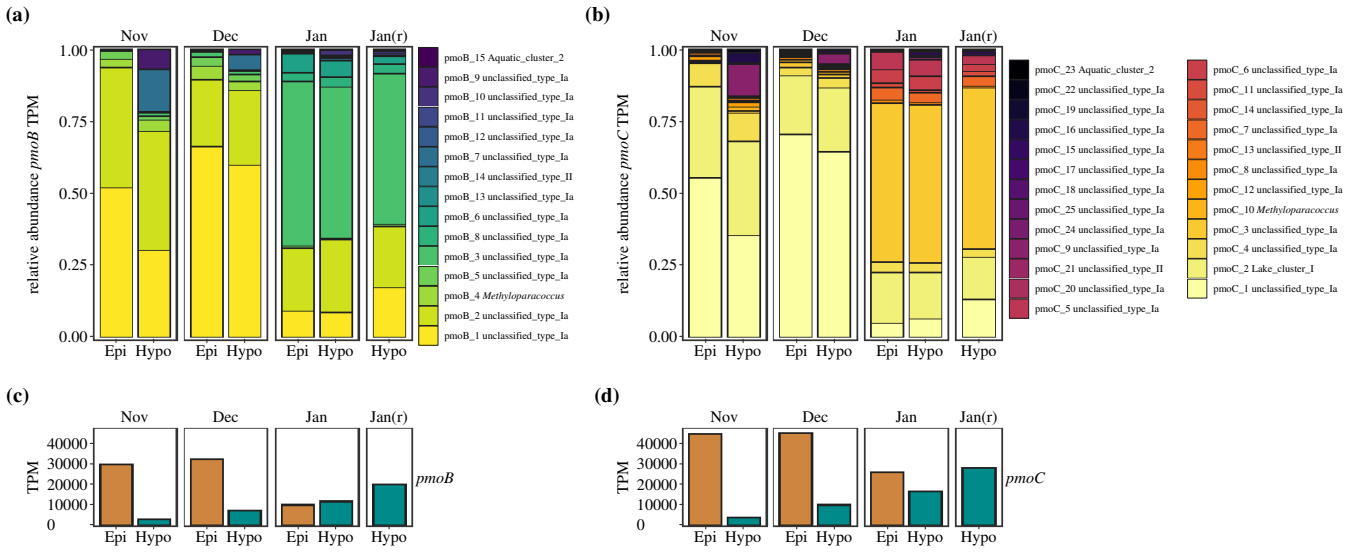

Supplementary Figure 3

Transcriptional activity of genes encoding pMMO in November, December and January 2017/2018 during overturn in Lake Rotsee. The hypolimnion sample in January was extracted twice and the replicate is labelled as "Jan (r)". Top panels show relative abundance of gene variants of (a) *pmoB* and (b) *pmoC* based on transcripts per million (TPM), mapped at 99% identity. *pmoB* and *pmoC* variants were assembled from metagenomic and metatranscriptomic samples originating from the same depths and dates as shown in Fig. 1. Different colour schemes were chosen for *pmoA* (Figure 3b), *pmoB* and *pmoC* variants. Bottom panels show relative importance of pMMO transcription in the transcriptome as summed TPM of all variants for epi- and hypolimnion (orange and cyan, respectively) for (c) *pmoB* and (d) *pmoC*. Epi = epilimnion, Hypo = hypolimnion.

Supplementary Tables

Supplementary Table 1

Summary of estimated parameters for Monod-kinetics of methane oxidation rates based on incubation experiments with natural water samples from above and below oxycline in Rotsee. Further, MOB cell numbers based on CARD-FISH data and *in-situ* measurements of methane oxidation rates are shown.

	October		November		December		January	
	Epilimnion	Hypolimnion	Epilimnion	Hypolimnion	Epilimnion	Hypolimnion	Epilimnion	Hypolimnion
Sampling date	10/10/2017	10/10/2017	23/11/2017	23/11/2017	07/12/2017	07/12/2017	09/01/2018	09/01/2018
Sampling depth (m)	2	10	4	13	4	13.5	4	15
K_m - Half-saturation constant (µM)	0.7	15.2	2.1	7.1	3.3	6.1	1.2	2.7
Standard deviation error for K_m	0.2	3.3	0.4	1.1	0.4	0.8	0.3	0.5
Distance of the 95% confidence interval around the optimal value for K_m	0.5	7.1	0.9	2.3	0.9	1.7	0.7	1.0
V_{max} per cell - Maximum cell-specific methane oxidation rate (fmol h^{-1} $cell^{-1}$)	1.8	0.8	8.4	0.6	4.7	1.6	0.8	0.9
Standard deviation error for V_{max}	0.2	0.1	0.5	0.0	0.2	0.1	0.0	0.0
Distance of the 95% confidence interval around the optimal value for V_{max}	0.4	0.2	1.2	0.1	0.4	0.2	0.1	0.1
a0 - Specific affinity (V_{max}/K_m) (10^{-12} L h^{-1} $cell^{-1}$)	2664	52	4170	83	1467	264	671	338
Standard deviation error for a0	813	12	774	13	195	36	169	52
Distance of the 95% confidence interval around the optimal value for a0	1875	26	1724	27	413	77	356	111
V_{max} - Maximum methane oxidation rate (µM h^{-1})	0.02	0.06	0.52	0.09	0.93	0.19	0.19	0.38
Standard deviation error for V_{max}	0.00	0.01	0.03	0.01	0.04	0.01	0.01	0.02
Distance of the 95% confidence interval around the optimal value for V_{max}	0.00	0.01	0.08	0.01	0.08	0.02	0.03	0.04
Degrees of freedom (number of samples minus one)	8	12	10	16	16	16	18	16
MOB cell numbers (10^5 cells mL^{-1})	0.1	0.8	0.6	1.5	2.0	1.2	2.5	4.3
Methane oxidation rate (µM h^{-1}) average of duplicates	0.01	0.11*	0.13	0.06	0.12	0.17	0.00	0.33

*single measurement

Supplementary Table 2

Transcripts per million (TPM) for *mmoX, mmoY, mmoZ,* which encode part of the soluble methane monooxygenase as generated from metagenomic and metatranscriptomics analysis. "MOB type" was determined by blasting (blastx) the gene against the NCBI protein_refseq database. Type Ia belong to *Methylococcales* (*Gammaprotebacteria*) as classified in Knief (2015). Epi=Epilimnion and Hypo=Hypolimnion. TPM of *mmoXYZ* showed a very low abundance throughout our sampling campaign. Fasta files are available at: https://doi.org/10.25678/0001fa.

gene					Transcripts per million						
MOB type	**variant**	**gene_id**	**contig**	**Length**	**Nov_Epi**	**Nov_Hypo**	**Dec_Epi**	**Dec_Hypo**	**Jan_Epi**	**Jan_Hypo**	**Jan_Hypo_rep**
mmoX											
type Ia	mmoX_1	CKCHICCI_119928	k141_374180_2	1584	0.9	0.1	0.9	0.3	0.1	0.0	0.3
type Ia	mmoX_2	CKCHICCI_614426	k141_2057240_1	1584	0.0	3.3	0.0	1.1	0.0	0.0	0.0
type Ia	mmoX_3	CKCHICCI_1871328	k121_2298038_2	1584	0.2	0.0	0.4	0.1	0.0	0.0	0.0
type Ia	mmoX_4	CKCHICCI_3043207	k121_5099499_1	1218	0.0	0.2	0.0	0.1	0.0	0.0	0.0
mmoY											
type Ia	mmoY_1	CKCHICCI_614427	k141_2057240_2	1179	0.0	2.2	0.0	1.0	0.0	0.0	0.0
type Ia	mmoY_2	CKCHICCI_1160907	k121_893959_4	1179	0.9	0.0	0.8	0.3	0.1	0.0	0.1
type Ia	mmoY_3	CKCHICCI_1871329	k121_2298038_3	1179	0.1	0.0	0.0	0.0	0.0	0.0	0.0
type Ia	mmoY_4	CKCHICCI_2602160	k121_4062417_1	570	0.0	0.1	0.0	0.0	0.0	0.0	0.0
mmoZ											
type Ia	mmoZ_1	CKCHICCI_207359	k141_653022_3	498	1.3	0.0	1.8	0.3	0.1	0.0	0.3
type Ia	mmoZ_2	CKCHICCI_1871331	k121_2298038_5	501	0.1	0.0	0.2	0.1	0.0	0.0	0.0
type Ia	mmoZ_3	CKCHICCI_2602162	k121_4062417_3	498	0.0	0.1	0.0	0.1	0.0	0.0	0.0

References

Knief, C.: Diversity and habitat preferences of cultivated and uncultivated aerobic methanotrophic bacteria evaluated based on pmoA as molecular marker, Front. Microbiol., 6(1364), 1–38, doi:10.3389/fmicb.2015.01346, 2015.

Kumar, S., Stecher, G. and Tamura, K.: MEGA7: Molecular evolutionary genetics analysis version 7.0 for bigger datasets, Mol. Biol. Evol., 33(7), 1870–1874, doi:10.1093/molbev/msw054, 2016.

Letunic, I. and Bork, P.: Interactive Tree Of Life (iTOL): An online tool for phylogenetic tree display and annotation, Bioinformatics, 23(1), 127–128, doi:10.1093/bioinformatics/btl529, 2007.

Oswald, K., Milucka, J., Brand, A., Littmann, S., Wehrli, B., Kuypers, M. M. M. and Schubert, C. J.: Light-dependent aerobic methane oxidation reduces methane emissions from seasonally stratified lakes, PLoS One, 10(7), 1–22, doi:10.1371/journal.pone.0132574, 2015.

Posch, T., Loferer-Krößbacher, M., Gao, G., Alfreider, A., Pernthaler, J. and Psenner, R.: Precision of bacterioplankton biomass determination: a comparison of two fluorescent dyes, and of allometric and linear volume-to-carbon conversion factors, Aquat. Microb. Ecol., 25(1), 55–63, doi:10.3354/ame025055, 2001.

Romanova, N. D. and Sazhin, A. F.: Relationships between the cell volume and the carbon content of bacteria, Oceanology, 50(4), 522–530, doi:10.1134/S0001437010040089, 2010.

Zimmermann, M., Mayr, M. J., Bouffard, D., Eugster, W., Steinsberger, T., Wehrli, B., Brand, A. and Bürgmann, H.: Lake overturn as a key driver for methane oxidation, bioRxiv, doi:10.1101/689182, 2019.